Journal of Polymers and the Environment
https://doi.org/10.1007/s10924-024-03263-z

ORIGINAL PAPER

Preparation and Characterization of SPEEK–PVA Blend Membrane Additives with Colloidal Silica for Proton Exchange Membrane Fuel Cell

Yavuz Yagizatli[1] · Berdan Ulas[2] · Alpay Sahin[1] · Irfan Ar[1]

Accepted: 23 March 2024

Abstract

An inexpensive membrane with high proton conductivity and high fuel cell performance, which can be an alternative to Nafion for PEMFC (Proton exchange membrane fuel cell), will overcome the obstacle to widespread commercialization of fuel cells due to high cost. For this purpose, SPEEK (sulfonated polyether ether ketone)-PVA (polyvinyl alcohol) blend membranes with colloidal silica additives were synthesized in this study. Ludox AS-40 was used as the colloidal silica source and the blend membrane was prepared by solution casting method. Water uptake capacity, swelling property, size change, dynamic mechanical analysis, ion exchange capacity, AC impedance analysis, hydrolytic and oxidative stability experiments of the synthesized Ludox additives blend membranes for fuel cell application were carried out, and the membranes were also characterized by FTIR (Fourier transform infrared) analysis. While the water uptake capacities of SPEEK/PVA membranes containing 1% Ludox, 5% Ludox, and 10% Ludox at room temperature were found to be 14.08%, 14.84%, and 16.6%, respectively, the water uptake capacities at 80ºC increased to 14.73%, 15.17%, and 17.11%. The proton conductivities of 1% Ludox, 5% Ludox and 10% Ludox doped SPEEK/PVA membranes at 80ºC were 0.25 S/cm, 0.56 S/cm, and 0.65 S/cm, respectively. Similarly, ion exchange capacities were determined to be 1.41 meq/g, 1.63 meq/g, and 1.71 meq/g, respectively. All Ludox-added membranes exhibited excellent hydrolytic stability, retaining approximately 88% of their mass after 650 h. In addition, in oxidative stability experiments carried out in 4 ppm Fe^{+2} at 80ºC, the 10% Ludox-added membrane exhibited the highest weight loss of 88.8% at the end of 24 h, while the 5% Ludox-additive membrane retained 91.6% of its total weight. Considering the proton conductivity and longevity tests of the synthesized membranes, they are thought to be promising structures.

Graphical Abstract

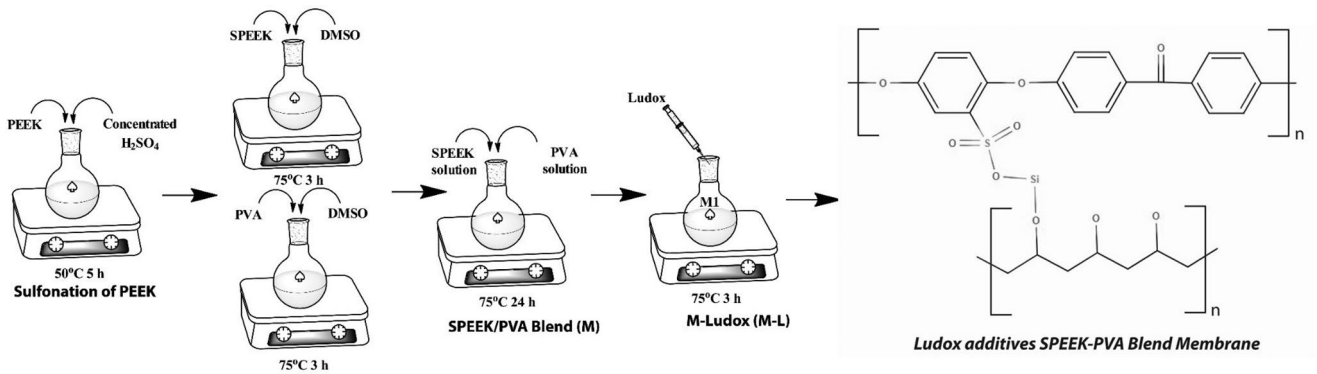

Keywords Ludox · SPEEK · PVA · PEMFC · Blend membrane

Extended author information available on the last page of the article

Introduction

Green and environmentally friendly alternatives are desperately needed in many fields, including energy [1]. Especially in the field of energy, the use of fossil fuels as an energy source causes greenhouse gas emissions and negatively affects human health and the environment [2–4]. Fuel cells are a great way to address the energy crisis because of their clean exhausts namely heat and water [5]. Fuel cells make it possible to access the energy contained in hydrogen, which is seen as the fuel of the future. Thus, fuel cells assist us in lowering our reliance on fossil fuels and other traditional fuels [6]. Fuel cells can be classified according to the type of electrolyte they contain [7]. Our focus is on polymer electrolyte membrane fuel cells due to their low operating temperature and versatility in both mobile and stationary applications [8]. The main obstacle to this kind of fuel cell's commercialization is its high cost of materials [9]. This problem can be solved by using substitute materials. Proton exchange membranes and catalysts are the main cost items for fuel cells [10]. Usually made of platinum-based catalysts, they are supported by any material with a large surface area. However, both adding a second metal to the catalyst system and reducing the catalyst loading rate are rational solutions that researchers are working on for lower-cost fuel cells.

Nafion is the most widely used proton exchange membrane, and it was created by DuPont [11]. It is a membrane made of perfluorosulfonic acid (PFSA) with hydrophilic ends and a Teflon backbone [12]. Although Nafion provides high proton conductivity, it is environmentally dangerous and expensive, so the development of alternative membranes is crucial for the commercialization of fuel cells [13]. Numerous polymers based on hydrocarbons are now being investigated in this regard. Due to its exceptional hydrophilicity, low cost, and ability to form films, polyvinyl alcohol (PVA) is one of these possibilities [14]. On the other hand, severe PVA membrane swelling is a serious problem since it can cause mechanical degradation [15]. Furthermore, there are no functional groups in pure PVA that could aid in proton transport [15]. To lessen swelling and enhance proton conductivity, partial crosslinking and reduction of free volume by the addition of organic or inorganic fillers are often employed methods [16]. On the other hand, it is also said that the membranes produced through the combination of two types of sulfonated polymers had excellent efficiency, a mixable structure, and elevated proton conductivity. Another polymer frequently reported in the literature as a proton exchange membrane is sulfonated polyether ether ketone (SPEEK) [17]. Because of their high degree of sulfonation, SPEEK membranes had a significant swelling ratio that ultimately reduced their mechanical strength [18]. Blending polymers is thought to be a useful technique for changing and enhancing the performance and characteristics of membranes.

Many fillers such as zirconium (Zr) [19–21], silicon dioxide (SiO_2) [22, 23], titanium dioxide (TiO_2) [24, 25], terephthalic acid (PTA) [26], molybdenum (Mo) [27], tungsten (W) [28], phosphorus (P) [29], aluminum (Al) [30], boron phosphate (BPO_4) [31], cerium oxide (CeO_2) [32], tin oxide (SnO_2) [33], etc. have been reported in the literature. Among these, colloidal silica (Ludox) is of interest due to its positive contributions to the membrane matrix. According to several studies, silica improves conductivity, reduces hydrogen crossing, and increases thermal stability in the polymer electrolyte membrane [34]. When hygroscopic silica is introduced to a polymer matrix, the bound water content and proton conductivity rise [35]. The porosity of silica increases the fuel used during the membrane reaction and contributes positively to fuel efficiency [36]. Additionally, it lowers the fuel crossover and enhances mechanical stability [37]. Ludox is defined as a colloidal silica and exhibits properties such as cost-effectiveness, high purity, long-term chemical stability, high dispersion, and uniform particle size distribution compared to that of conventional silica. Therefore, they are promising inorganic fillers for fuel cell membranes.

In this study, we investigate how the addition of Ludox to SPEEK-PVA membranes affects the membranes' ability to absorb water, exchange ions, conduct proton flow, and chemical stability, among other characteristics. SPEEK-PVA-Ludox material as a proton exchange membrane for PEMFCs has not yet been reported in the literature, and this work is novel in this respect.

Materials and Methods

In the scope of the study, the membrane main matrix consists of SPEEK and PVA. SPEEK is obtained as a result of the sulfonation of PEEK (polyoxy-1,4-pheneyleneoxy-1,4-pheneylene carbonyl-1,4 phenylene, %99.999 purity). PEEK used to obtain SPEEK has 20,800 M_w and was supplied from Aldrich. The other main matrix, PVA, has 99% purity and M_w ranging from 85,000 to 124,000 and was provided by Merck. Ludox (AS-40 colloidal silica), used in the membrane matrix as an additive material, was obtained from Merck and is 40% suspended in water by weight. Sulfuric acid (H_2SO_4, 96% purity) obtained from Aldrich was used as the sulfonation agent in PEEK sulfonation. Dimethyl sulfoxide (DMSO, ≥%99.9 purity), an organic solvent with 99% purity purchased from Merck, was used as the solvent in the synthesis studies. In the Fenton solution prepared to determine the oxidative stability of membranes, hydrogen

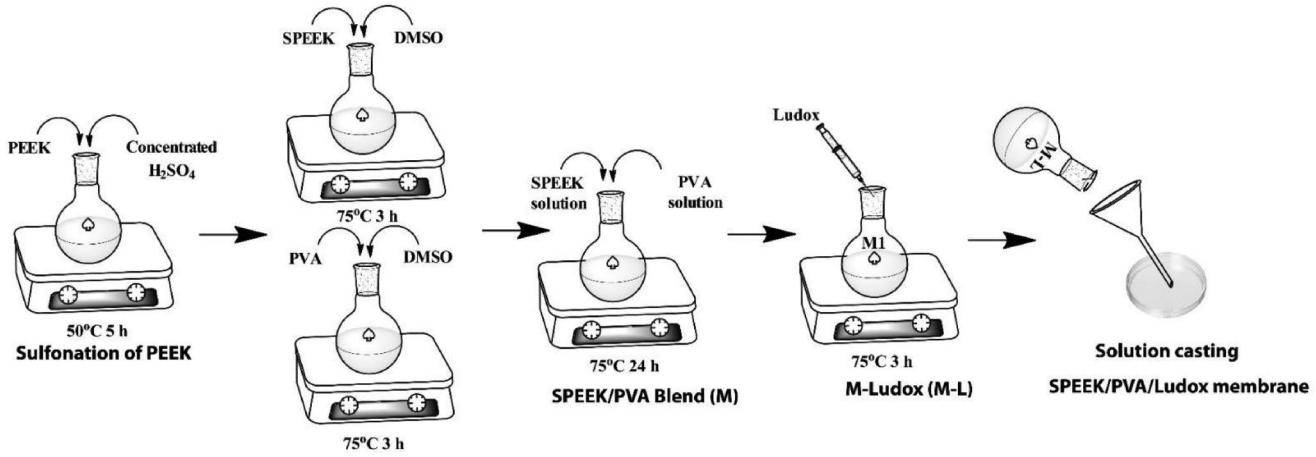

Fig. 1 A schematic representation of the synthesis procedures

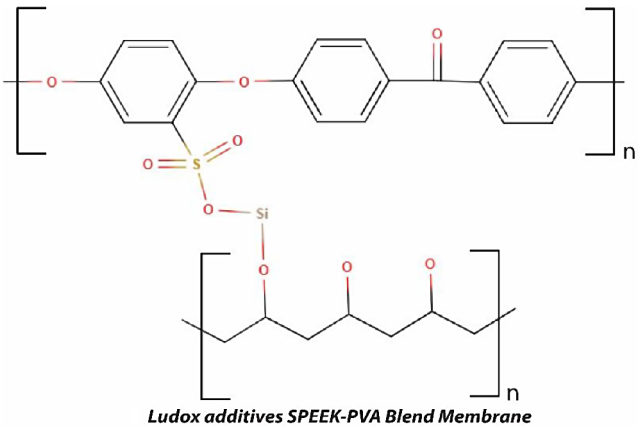

Fig. 2 Possible chemical structure of Ludox doped blend membrane

peroxide (H_2O_2, 30%) obtained from Aldrich and Iron(II) sulfate heptahydrate ($FeSO_4.7H_2O$, >%99 purity) as the Fe^{+2} source obtained from Merck were used. Nafion-117 (thickness: ∽177.8 µm, basis weight: 360 g/m^2), purchased from Ion Power, was used as a commercial membrane for comparison with the synthesized membranes.

Blend Membrane Synthesis

For the Ludox-additive SPEEK-PVA blend membrane synthesis, SPEEK polymers were first obtained through PEEK sulfonation. The sulfonation process performed to obtain SPEEK polymers was explained in detail in our previous study [38]. The sulfonation degree of SPEEK polymers obtained by the sulfonation process was determined to be 57%. Blend membrane synthesis was carried out using the solution casting method. SPEEK and PVA polymers were dissolved in DMSO under continuous stirring at 20% w/v. The resulting homogeneous PVA solution was poured onto the SPEEK solution and continued to be mixed until a homogeneous solution was obtained. On the other hand, the specified amount of Ludox (1%, 5%, and 10% by weight) was dissolved in DMSO under constant stirring. After the homogeneous solutions were formed, the solution containing Ludox was added to the blend membrane solution, and mixing continued. The solution was mixed for one day, placed in Petri dishes, and kept in the oven (24 h at 40°C on the first day, then at 60°C) until it formed a membrane. A schematic representation of the synthesis procedures of membranes is given in Fig. 1. Finally, thermal cross-linking was applied to the synthesized membranes in order to increase their stability in water. For thermal crosslinking, the membranes were sandwiched between two glasses and exposed to 180°C. The possible chemical structure of the Ludox additive SPEEK-PVA blend membrane is given in Fig. 2. The thickness of the synthesized membranes was found with the help of a digital thickness gauge and was 89 ± 2.2 µm, 93 ± 1.8 µm, and 101 ± 2.3 µm, respectively, with increasing Ludox ratios.

Characterization Studies

Fourier transform infrared (FTIR), water uptake capacity (WUC), swelling property (SP), size change (SC), dynamic mechanical analysis (DMA), ion exchange capacity (IEC), AC impedance analysis (EIS), hydrolytic stability and oxidative stability studies were carried out with the synthesized Ludox additive SPEEK-PVA blend membranes. X-ray diffraction (XRD) analyses were conducted to evaluate the presence of amorphous or crystalline phases and assess the efficacy of membrane synthesis. XRD measurements were carried out utilizing the Rigaku D/MAX 2200 instrument, with a scanning range from 2 to 90 degrees and a scan rate of 2 degrees per minute. Thermal gravimetric analysis coupled with derivative thermogravimetry (TGA-DTA) was employed to examine the thermal stability of the synthesized membranes and ascertain weight loss

tendencies with increasing temperature. These investigations were performed using the Setaram Labsys system, with a temperature range from 30 to 900 °C and a heating rate of 10 °C per minute. DSC analysis was also performed to determine the membrane's glass transition temperature and thermal strength. DSC analyses were performed on an AHP DSC 500 model device at an N_2 flow rate of 50 mL/min, a heating rate of 10°C/min, and a temperature range of 50-250°C. Using a Zeiss VP Sigma 300 FESEM, a field emission scanning electron microscope was used for high-resolution surface images of the membranes. The 10 kV accelerating voltage (EHT) for the In-Lens (SE1) detector was established on the FESEM. Using a SE2 detector, elemental mapping and energy dispersive X-ray (EDX) were recorded at 20 kV. FTIR measurements were conducted using Bruker brand VERTEX 70v model FT-IR spectrophotometer device between 400 and 4000 cm^{-1} wave numbers, using ATR apparatus and MIR detector. For WUC, SP, and SC experiments, membranes were cut to 2 cm × 2 cm and dried. The weights of dry membranes were measured on a sensitive scale for WUC, their thickness was measured with a SHEEN thickness gauge for SP, and membrane areas were measured with a digital caliper. The membranes were kept in water at room and 80°C temperatures for one day. Membranes were removed from the water at the end of the day, their weights, thicknesses, and areas were measured and the WUC, SP, and SC properties of the membranes were calculated, respectively, with the help of the following Eq.

$$WUC\,(\%) = \frac{W_W - W_D}{W_D} \times 100 \tag{1}$$

$$SP\,(\%) = \frac{T_W - T_D}{T_D} \times 100 \tag{2}$$

$$SC\,(\%) = \frac{A_W - A_D}{A_D} \times 100 \tag{3}$$

Herein, W and D, given as subscripts, indicate wet and dry properties, respectively. The symbols W, T, and A represent the weight, thickness, and area of the membrane, respectively.

DMA was carried out with a Shimadzu brand mechanical resistance analyzer with a crosshead speed of 3 mm/minute. Before the mechanical strength tests, the membranes were cut to the specified dimensions and then kept in pure water to determine the strength under real fuel cell conditions. Maximum tensile strength, elongation at break, and Young's modulus values of the membranes were obtained with DMA. In IEC experiments, three membranes of equal size were cut and dried in the oven. The weight of the dried membranes was measured and subjected to protonation. During protonation, the membranes were kept in sulfuric acid one day and in pure water the next day. Protonated membranes were kept in sodium chloride (NaCl) solution for two days. Then, the solution was titrated with sodium hydroxide (NaOH) solution and the titrant amounts were recorded. The titration process was carried out on a Schott brand TA500 plus model device at a titrant flow rate of 2 mL/min. The IEC of membranes was calculated with the help of the formula below.

$$IEC\,(meq/g) = \frac{V_t \times, M_{w,t}}{W_D} \tag{4}$$

Here, t used as the subscript represents the titrant, V symbolizes the titrant volume and M symbolizes the molecular weight of the titrant.

EIS analyses were performed to determine the proton conductivities of the membranes. The resistances of the membranes were obtained from the Nyquist diagrams obtained from EIS analysis and proton conductivity values were calculated with the help of Eq. 5. EIS measurements were carried out at two different temperatures, room and 80°C, and an acidic electrolyte environment (0.05 M H_2SO_4, %100 RH) with the CH instruments model 600 series.

$$\sigma\,(S.cm^{-1}) = \frac{L}{R \times, W \times, T} \tag{5}$$

Here, L is the distance between the electrodes, R is the membrane resistance and W is the membrane width.

The dried and weighted membranes were immersed in pure water for the hydrolytic stability test. The membranes were removed from the water at certain periods and kept in the oven at 100°C until they dried and their weights were recorded. The membranes, whose dried weights were measured, were immersed in water again and the hydrolytic stability test was continued for 650 h. The oxidative stability of the membranes was determined by the Fenton test. Similar to the hydrolytic stability experiment, membrane pieces cut into appropriate sizes were dried and weighed. Then, it was immersed in Fenton's agent containing 3% hydrogen peroxide and 4 ppm Fe^{+2} by weight at 80°C. At certain intervals, the membrane pieces removed from the Fenton agent were dried at 100°C and weighed again. This process was repeated several times and the oxidative stability of the synthesized membranes was obtained.

The synthesized membranes are coded as shown below Fig. 3.

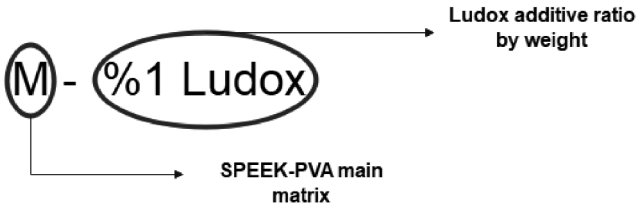

Fig. 3 Example illustration of material coding

Results and Discussions

FTIR Analysis

Figure 4 presents the FTIR spectra of 1% Ludox, 5% Ludox, 10% Ludox, pure PVA, and pristine SPEEK membranes. The peaks observed at 3300 cm^{-1} are attributed to intramolecular hydrogen bonds. The peaks between 2840 and 3000 cm^{-1} are due to C-H stretching of alkyl groups. C=O streching vibration of PVA was detected between 1710 and 1750 cm^{-1}. The peaks detected between 1080 and 1200 cm^{-1} are assigned to C-O-C stretching [39]. The O–H stretching vibration of sulfonic acid groups is observed at 3425 cm^{-1}. On the other hand, as expected, due to its hydrophilic structure, the most intense peaks representing hydroxyl groups, located between 3200 and 3400 cm^{-1}, belong to PVA. A significant decrease in the peak intensities in this region was observed due to the thermal crossover process performed on Ludox additive membranes and the involvement of OH groups in this thermal crosslinking reaction [40]. However, as the ratio of the hydrophilic Ludox contribution in the membrane matrix increased, the intensities of the peaks representing OH groups increased. Observed bands at 1080 cm^{-1}, 1220 cm^{-1}, 710 cm^{-1}, and 1024 cm^{-1} could be attributed to symmetric O=S=O, asymmetric O=S=O, S-O stretching, and S=O stretching vibration of SPEEK [41]. In addition, the bands observed at 472 cm^{-1} and 803 cm^{-1} wavenumbers of Ludox-added membranes indicate Si-O-Si bending vibration [42, 43]. . The characteristic peaks of SPEEK and PVA, concentrated in the 500–1750 cm^{-1} range, obscured the other peaks of Ludox. The detection of the main characteristic peaks of SPEEK, PVA, and Si indicates that SPEEK/PVA/ Ludox membranes were successfully synthesized.

Crystallographic Properties of M-Ludox

Figure 5. shows the XRD patterns of M-10% Ludox and M-1% Ludox membranes. The diffraction peaks of PEEK at approximately 19°, 21°, 23°, and 29° 2Θ angles reported in the literature disappeared as a result of the sulphonation reaction and thermal crosslinking process. With the entry of $-SO_3H$ groups into the membrane matrix, a broad peak was observed at 20.56° 2Θ angle for M-10% Ludox and M-1% Ludox membranes [44, 45] (Fig. 5a). The peaks detected at 19.16°, 19.98° and 23.0° 2Θ angles were attributed to the (1 0 $\bar{1}$), (1 0 1) and (2 0 0) facets of PVA, respectively [46] (Fig. 5c). In addition, the diffraction peak detected at 44.50° corresponds to the compound peak consisting of (111), (1$\bar{1}$ 1), (210), and (2$\bar{1}$ 0) planes [47]. Particularly, the diffraction peaks observed at 25.9° and 57.46° 2Θ angles in the XRD pattern of the M-10% Ludox membrane were assigned to the Si (1 0 1) and Si (1 0 3) planes [48] (Fig. 5b and c). The observation of Si diffraction peaks in the XRD patterns of the Ludox content membranes indicates that the inorganic doping was successfully carried out.

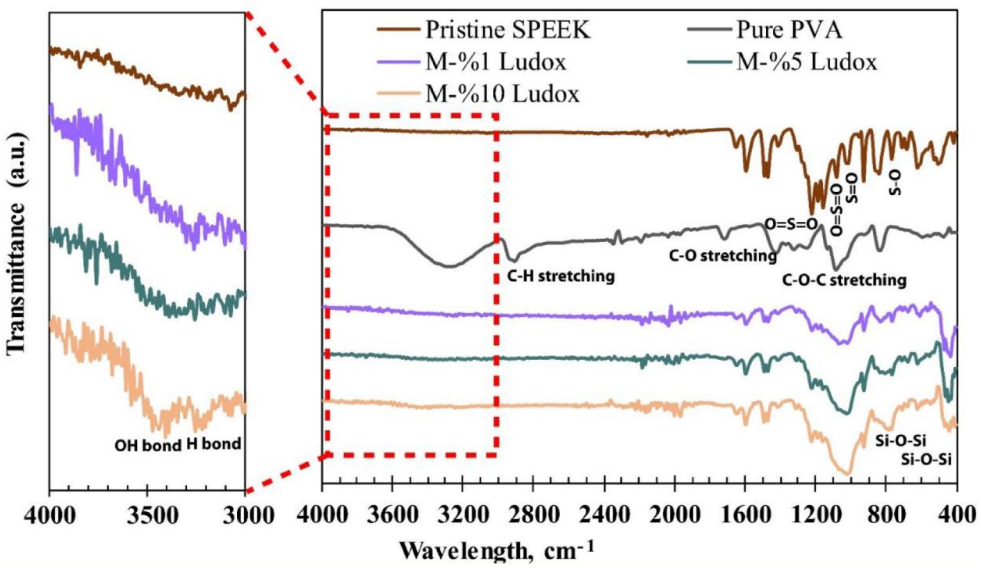

Fig. 4 FTIR spectra of %1 Ludox, %5 Ludox, %10 Ludox, pure PVA, and pristine SPEEK

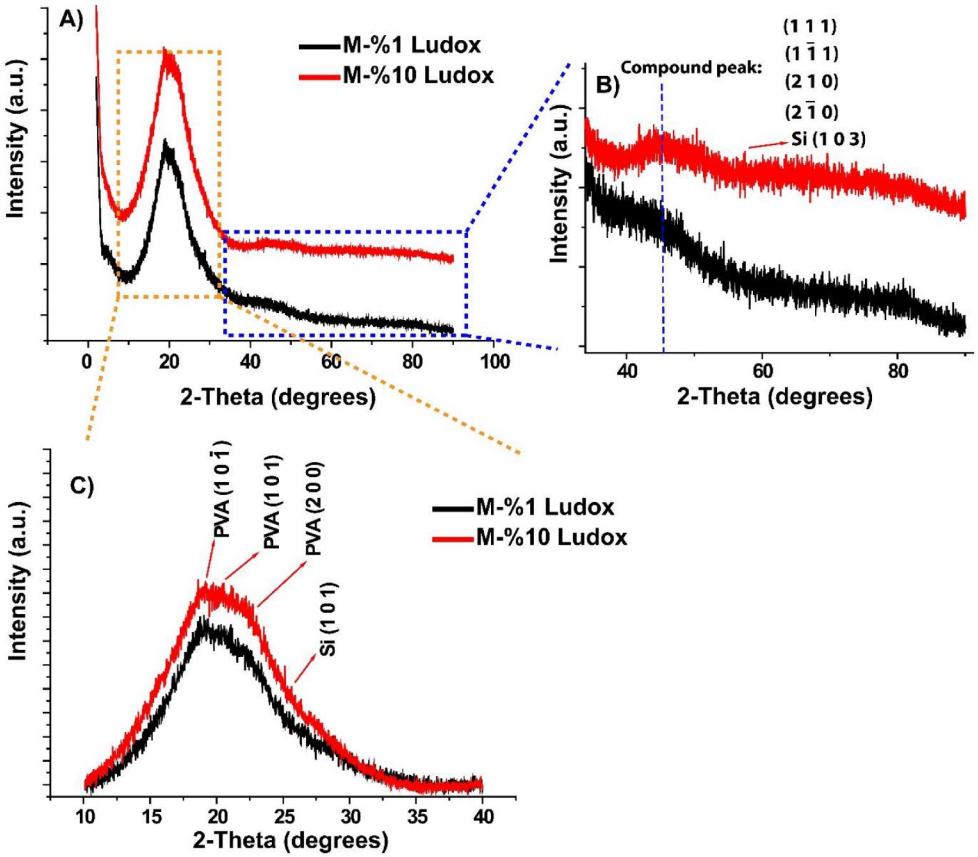

Fig. 5 XRD pattern for M-%1 Ludox and M-%10 Ludox between 2Θ angle of (**a**) 0–90°, (**b**) 35–85°, and (**c**) 10–40°

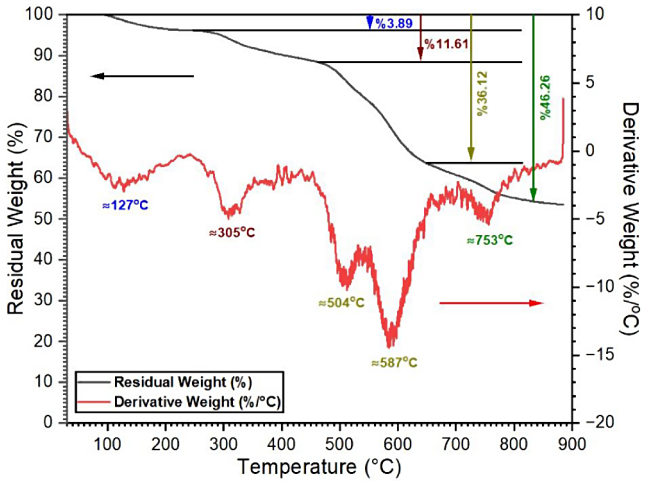

Fig. 6 TGA-DTA thermogram of M-10% Ludox membrane

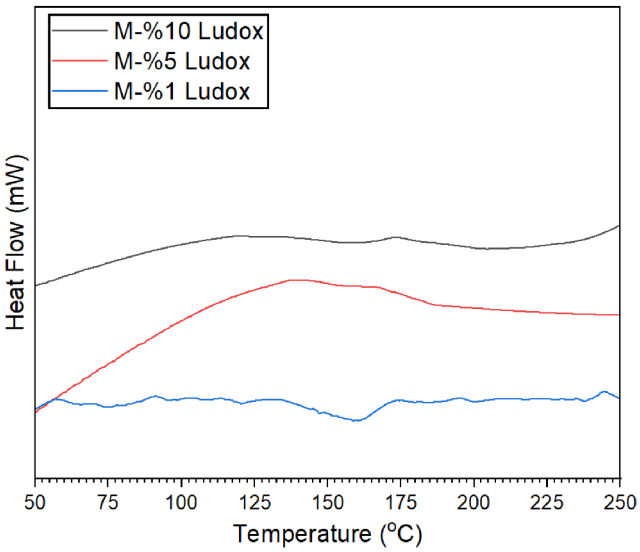

Fig. 7 DSC thermogram of Ludox additive membranes

Thermal Properties of M-Ludox

In order to determine the thermal properties of the Ludox-doped membrane, TGA-DTA was performed with the M-10% Ludox-coded membrane. The TGA-DTA thermogram of the M-10% Ludox membrane is given in Fig. 6. In addition to TGA-DTA, DSC analyses were carried out to determine the glass transition temperatures and thermal behavior, and the DSC thermograms of the membranes are given in Fig. 7.

In the TGA thermogram, it is seen that there are four major weight losses. The first weight loss started at approximately 100°C and continued until 160°C. Here, the membrane lost 3.89% of its mass. The weight loss between these

temperatures is due to the physical adsorption or removal of molecular water resulting from moisture on the surface [49, 50]. In addition, Ludox (SiO_2) is known to have a very thermally stable structure. Weight loss of Ludox generally occurs up to 200°C and exhibits < 5% weight loss of its total [51–53]. For this reason, Ludox also slightly affects this weight loss. The second weight loss occurred between temperatures of 240-460°C, and there was a loss of 11.61% in the weight of the membrane between these temperatures. The loss between these temperatures is due to the desulfonation of sulfonic acid groups, degradation of the side, and the partially main chain of PVA [54]. The third, largest weight loss occurred between temperatures of 465-640°C, and a two-step decomposition was observed. At the end of this temperature, the total weight loss in the membrane reached 36.12%. The main reasons for the mass loss here are due to the massive degradation of the main chain of PVA and SPEEK [55, 56]. The final weight loss centered at 753°C indicates the degradation of the membrane main matrix. It was determined that 53.59% of the membrane weight was preserved at the end of 900°C temperature. In general, it has been determined that the synthesized membrane has a very thermally stable structure at 80°C, which is the PEMFC operating temperature, and beyond that, its use in high-temperature fuel cells is possible due to its thermal properties.

It was determined from DSC thermograms that all synthesized membranes had a very stable structure. In addition, it was determined that as the Ludox ratio increased in the membrane structure, the glass transition temperatures of the membranes increased slightly. While the glass transition temperature of the M-1% Ludox coded membrane is approximately 166°C, the glass transition temperature is approximately 168°C and 170°C with increasing Ludox ratios, respectively. The additive material Ludox (mainly composed of silica), which has a high glass transition temperature, caused an increase in the glass transition temperature of the membrane, which is parallel with the studies in the literature [57, 58]. In addition, it was determined that the glass transition temperatures of the synthesized membranes were higher than the fuel cell operating temperature and that the proton conduction mechanism obeyed an Arrhenius-type law, which positively affected proton conduction [59].

Morphology of M-Ludox

To examine the morphology of the Ludox-doped membrane, SEM-EDX, and elemental mapping analyses were carried out with the M-10% Ludox coded membrane. SEM images, EDX results, and elemental mappings of the synthesized M-10% Ludox membrane are given in Fig. 8.

SEM imaging was performed from the lateral cross-sectional area and the upper surface of the membrane. It can be seen from both SEM imaging and elemental mapping that the Ludux contribution is distributed homogeneously within the membrane matrix. Additionally, it was determined that a non-porous structure was formed as desired. Besides, Fig. 9-e, agglomeration has started in certain areas. It can be seen that a small amount of accumulation has formed in the areas where the channels are located. In elemental mapping, carbon comes from both SPEEK and PVA, sulfur comes from SPEEK, and silicon comes from the additive material Ludox. As can be clearly seen, there is a homogeneous distribution in all of them and no intense accumulation in a particular region. In SEM analyses, it was determined that the desired structure was successfully synthesized.

Water Uptake and Swelling Properties of M-Ludox

The composite membranes' water uptake capacity is a crucial factor for membrane performance toward PEMFC. Proton conductivity, hydrolytic stability, and mechanical stability of PEM are all impacted by water uptake capacity. Figure 9 shows the water uptake values of SPEEK/PVA/Ludox and Nafion-117 membranes at room temperature and 80°C. The room temperature water uptake capacities of SPEEK/PVA membranes containing 1% Ludox, 5% Ludox, 10% Ludox, and, commercial Nafion-117 were found to be 14.08%, 14.84%, 16.6%, and 23.84%, respectively. At 80°C, the water uptake capacities were determined as 14.73%, 15.17%, and 17.11% with the order of increasing Ludox amount. The increasing water uptake capacity with increasing Ludox amounts at both temperatures can be explained by the hygroscopic nature of Ludox. It was also observed that the water uptake capacity of membranes increased with the increase in temperature from room temperature to 80°, and this phenomenon can be explained by the boosting of ionic mobility with increasing temperature. Sahin reported that ionic conductivity improved with increasing temperature as a result of increasing ionic mobility and the number of water molecules entering into free volumes of the membrane matrix [60].

Changes in thickness of 1% Ludox, 5% Ludox, 10% Ludox, and Nafion-117 membranes were 5.25%, 4.59%, 4.23%, and 9.19% at room temperature and 4.44%, 2.02%, 3.92%, and 10.68% at 80°C, respectively (Fig. 3b). It was found that the swelling rate decreased as the increased Ludox additive entering the membrane matrix (Fig. 7c). Although higher water uptake capacity was obtained with increasing Ludox content, the slightly decreased swelling value was explained by the fact that Ludox imparts flexibility to the SPEEK-PVA blend membrane. Therefore, it is concluded that the mass transfer resistance will decrease with increasing Ludox ratio.

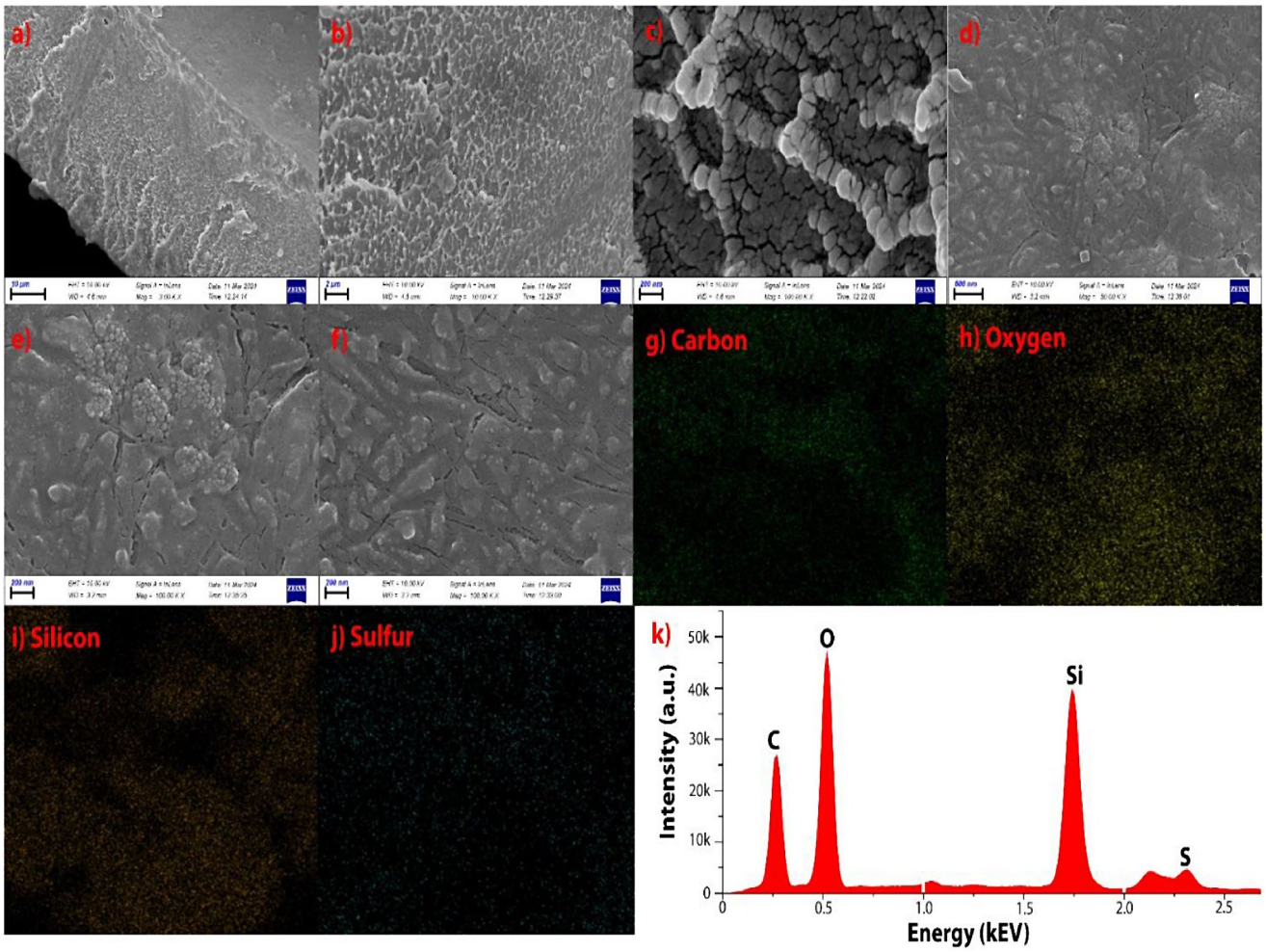

Fig. 8 **a-f**) SEM images, **g-j**) elemental mapping, and **k**) EDX results of M-%10 Ludox membrane

In our previous studies carried out by our research group, the water uptake capacities of pristine SPEEK and SPEEK/PVA were determined as 18.18% and 19.17% at room temperature, while they were reported as 23.2% and 20.45% at 80°C [38, 40]. With the introduction of Ludox inorganic additives into the structure, a decrease in water uptake capacity was detected both at room temperature and at 80 °C. The fact that the water uptake capacity of the M-Ludox membrane is lower than that of pristine SPEEK is a natural result of the thermal crosslinking process. On the other hand, due to a higher degree of thermal crosslinking with the inorganic material, the molecular space within the membrane matrix decreased, and as a result, water uptake decreased in Ludox-doped membranes compared to SPEEK/PVA blend membranes.

Dynamic Mechanical Analysis

During installation and operation, fuel cell membranes are subjected to mechanical stresses. This is particularly important for thin membranes since a rupture during operation could result in a catastrophic failure [61]. Therefore, the DMA of Nafion-117 and the synthesized membranes were performed and are shown in Fig. 10. When the Ludox doping rate was increased from 1 to 5%, the tensile stress value increased from 30.82 MPa to 38.86 MPa. When the doping rate was increased up to 10% Ludox, it was observed that the tensile stress decreased to 26.79 MPa. It is concluded that the decrease in tensile stress may be due to hydrogen bonding between Ludox and SPEEK/PVA [60]. In addition, the decreased mechanical strength of Ludox-doped membranes compared to pristine SPEEK and SPEEK/PVA membranes proves this situation [38, 40]. A more rigid and brittle membrane was obtained, especially at a 10% Ludox doping ratio [62]. The elongation at break values of Ludox-added SPEEK/PVA membranes showed a similar trend with the tensile stress values. It was determined from the elongation at break values that the membrane became stiffer and its ductility decreased with increasing Ludox doping. On the other hand, there is a significant difference in the elongation

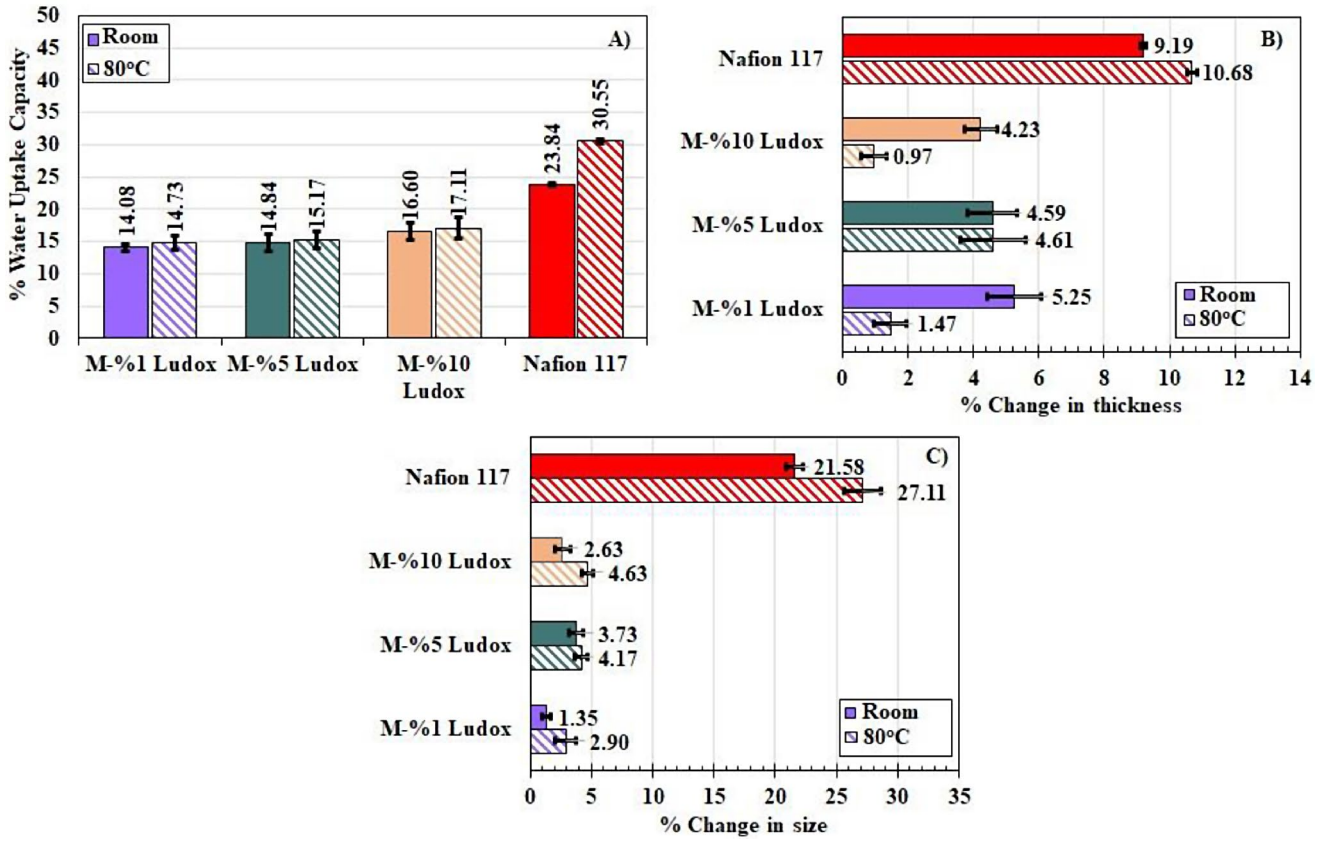

Fig. 9 (**a**) Water uptake capacity, (**b**) change of thickness, and change of thickness of %1 Ludox %5 Ludox, %10 Ludox and Nafion-117

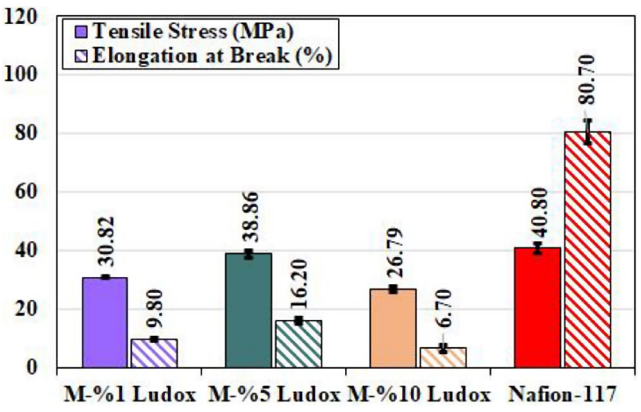

Fig. 10 DMA results of %1 Ludox, %5 Ludox, %10 Ludox, and Nafion-117

at break values of Ludox-doped membranes compared to Nafion-117. This is a natural consequence of thermal crossover, except that Nafion is highly elastic. As a result of the formation of solid and rigid intermolecular bonds after thermal crossover, the membrane's flexibility decreased. However, elasticity is not vital for a membrane to be used in a fuel cell, as the membrane must withstand the pressure difference that may occur on the anode and cathode sides of the fuel cell. What is more critical here are the tensile stress values. With the results obtained, the tensile stresses of the synthesized membranes have very close values compared to the commercial membrane. In a study conducted by Wang et al., it was stated that SiO_2 additive membranes had strains ranging from 24.9 to 34.4% and tensile stress values ranging from 41.3 to 52.9 MPa. It has been reported that the tensile stress decreased almost four times after thermal treatments and phosphoric acid doping [63]. In another study where SiO_2 additive material was used in the membrane matrix, it was stated that the elongation at break values of SiO_2 additive membranes varied between approximately 10%-7.5%, and the tensile strength varied between approximately 42 – 40 MPa [64]. In another SiO_2-based study, it was reported that elongation at break values decreased with increasing SiO_2 amounts in the membrane matrix, elongation at break values decreased from approximately 3.8–2.4% with increasing SiO_2 ratios, and tensile stresses varied between approximately 37 MPa and 28 MPa [65]. It was concluded that the prepared Ludox-added membranes are suitable for use as membranes in PEMFCs in terms of their mechanical properties since they have both stiffness and ductility [66].

Ion Exchange Capacity

IEC, an important measure of proton conductivity, was carried out to determine the presence of ion-exchangeable groups in the synthesized membranes. IEC and hydration degrees obtained with the synthesized membranes and Nafion-117 are given in Fig. 11.

It was determined that the IECs of the membranes increased as a result of the increase in the amount of Ludox in the membrane matrix. Moreover, all of the synthesized membranes had higher IECs compared to Nafion-117. The IEC trend in the synthesized membranes is similar to the water uptake capacities. In some of the studies carried out in the literature using silica sources, it has been reported that IECs decrease due to the decrease in ion exchange groups as a result of the increase in silicon sources in the membrane structure [67, 68]. Here, in Ludox-additive membranes, the opposite of this situation exists. The interaction and functionalization of the sulfonic groups with the additive Ludox led to the improvement of the IECs of the membranes [69]. The parallel increase in IEC with Ludox is caused by the formation of more acidic groups due to the strong interaction of SiO_2-SO_3H groups in the blend membrane and the change in the crystallinity of the membrane [70]. In our previous study, it was determined that while 1.722 meq/g IEC was obtained with pure SPEEK, this value decreased to 1.35 meq/g with SPEEK/PVA membrane [38, 40]. With the addition of PVA to the structure, the decrement in active sulfonic acid groups per unit volume in the membrane matrix forms the basis of this decrease. With the addition of Ludox, the IEC of the membranes increased and compensated for the decrease in the density of sulfonic acid groups in the structure. On the other hand, the higher uptake capacity of the membranes may have led to the formation of new ion exchange groups. Using WUC and IEC values, the hydration numbers of the membranes were obtained with Eq. 7.

$$\lambda = \frac{WU}{IEC} \times \frac{10}{18} \tag{7}$$

The degree of hydration is one of the factors affecting membrane performance and is defined as the number of water molecules adsorbed per unit volume of -SO_3H groups. Since protons move with the help of water molecules in the fuel cell, it is expected that the proton conductivity will be enhanced by the water molecules in the membrane structure if the degree of hydration is higher. Contrary to IEC values, Nafion-117 has a much higher hydration degree than the Ludox-added membrane. Although the highest hydration degree at both temperatures (room and 80ºC) was achieved with a 1% Ludox-additive membrane among synthesized membranes, these values are approximately three times less than Nafion-117 under the same conditions. Nafion-117 has a much higher WUC than the synthesized membranes. Having a high WUC ensures the membrane has a high hydration degree. Although Ludox additive blend membranes have more ion-exchangeable groups, it is clear that the degree of hydration has a very important role in the proton transfer that takes place with the help of water molecules.

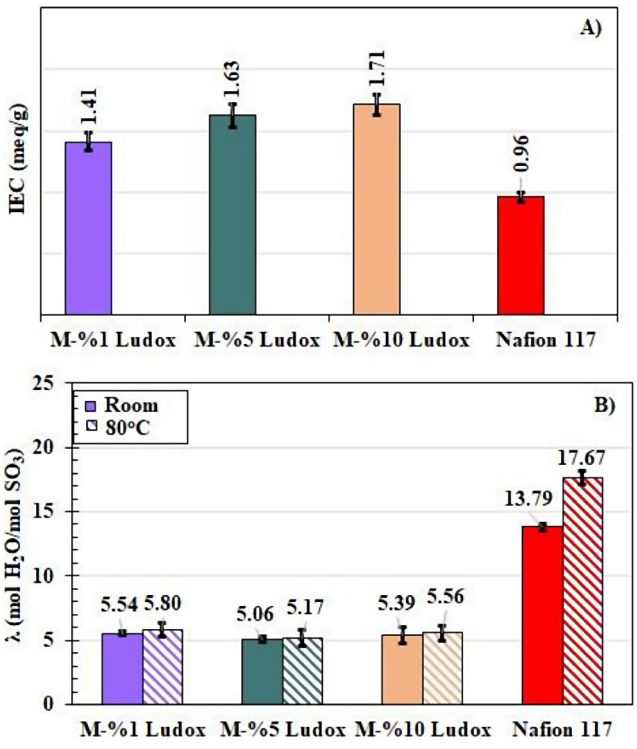

Fig. 11 (**a**) IEC and (**b**) hydration degrees of synthesized membranes and Nafion-117

AC Impedance Analysis

AC impedance analyses were carried out to determine the proton conductivities of the synthesized membranes. Proton conductivity results and Nyquist diagrams are given in Fig. 12.

As the Ludox additive ratio and temperature increased, the proton conductivities of the membranes enhanced. Together with the increasing temperature, ionic conductivity improved, membranes became more elastic, and proton conduction became easier, which led to an increase in the proton conductivity of the membrane. Colloidal silica in Ludox is recognized for its hygroscopic properties and it can absorb water. This proves advantageous for enhancing the proton conductivity of the membrane [71]. It was observed that the Ludox additive made a positive contribution to proton conductivity compared to pristine SPEEK (0.414 S/cm) and SPEEK/PVA (0.195 S/cm) [38, 40]. The main reason for this situation, as mentioned in the IEC

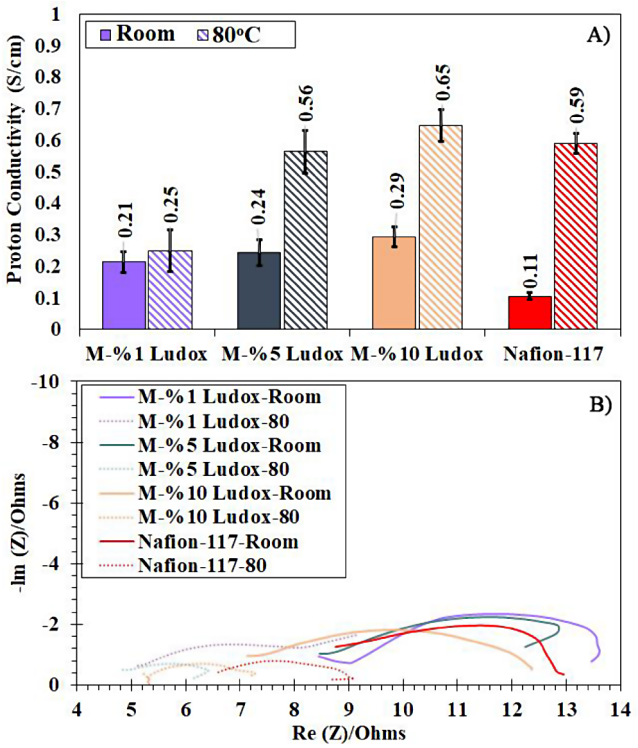

Fig. 12 (**a**) Proton conductivities, and (**b**) Nyquist diagrams of the synthesized membranes

analysis, is due to the strong interaction between -SO_3H and SiO_2, and this interaction creates new proton conduction channels. In most of the studies carried out in the literature, it has been stated that there is an improvement in proton conductivities by incorporating silica-based additive materials into the membrane structure [72–76]. In the study conducted by Xie et al., they stated that the mesoporous structure increased the proton conductivity as a result of the proton conductivity experiments carried out by using the silica additive material [75]. In another study, researchers concluded that silica-based additives increased the water uptake capacity and proton conductivity of the SPEEK-based membrane even at low relative humidity, and this was due to silica-based structures [76]. Yang et al., who carried out studies on PVA/SiO_2 membrane, stated that proton conductivity increased up to 10% SiO_2 additive by weight [77]. As a result of the increase in water uptake capacity, the formation of new proton conduction channels and the strong interaction of sulfonic acid groups, which are active groups in proton transport, with SiO_2 enabled the improvement of proton conductivity. Traces of this interaction can also be seen in size and thickness changes. The strong interaction limited the size and thickness changes in the membrane. It is seen that Ludox-additive membranes, which have almost no change compared to Nafion-117, will be less affected by mass transfer resistances, and this will have a positive impact on both proton conduction and fuel cell performance. As a result, with the increase in the Ludox ratio, the increase in the peak intensities of the active groups in the FTIR spectra, water uptake capacity, and IEC value had a positive effect on the proton conductivity, and the highest proton conductivity value was obtained with the M-10% Ludox coded membrane. Therefore, FTIR, water uptake capacity, and IEC values are descriptive of high proton conductivity values for all membranes as expected.

Water uptake capacity results show that the membranes absorb more water molecules with increasing Ludox amounts. A significant correlation was detected between the water uptake capacity and proton conductivity of Ludox-doped membranes at 80°C. Therefore, although free water decreases at high temperatures, proton conductivity increases with increasing Ludox amounts, indicating that proton conduction proceeds by the Grotthuss mechanism at high temperatures. The chemical phenomenon that triggers the Grotthuss mechanism is thought to be the hydrogen bond between the –OH group in the polymer matrix and the Si in the Ludox structure [78]. No significant differences were observed between the proton conductivities of M-1% Ludox, M-5% Ludox, and M-10% Ludox membranes at room temperature. Accordingly, it was noteworthy that the proton conductivity values at room temperature were close to each other (0.21, 0.24, and 0.29 S/cm for M-1% Ludox, M-5% Ludox, and M-10% Ludox). Therefore, it was concluded that proton conduction at room temperature proceeds through the vehicle mechanism with the free water in the membrane content [79]. As a result, when IEC, water holding capacity, and proton conduction results were evaluated together, it was concluded that proton conduction proceeded by the vehicle mechanism at room temperature and by Grotthuss mechanisms at 80°C.

Several SPEEK/PVA-based membranes for PEMFCs have been reported in the literature. In a study conducted by our working group, SPEEK/PVA membranes were prepared, and it was determined that with the introduction of PVA into the structure, the density of sulfonic acid groups decreased and membrane elasticity increased [40]. In the study conducted by Sahin, the negative effect of decreasing sulfonic acid groups on proton conductivity was compensated by the TEOS additive, and a proton conductivity of 0.085 S/cm was reported. The increased performance of the membrane was attributed to the increase in oxidative and hydrolytic resistance of PVA and TEOS additives [60]. It was reported by Rodriguez et al. that the proton conductivity of SPEEK/PVA membranes doped with GO increased with increasing temperature. The fact that the membrane performance does not decrease at relatively high temperatures such as 130°C and the proton conductivity of 0.083 S/cm is achieved is attributed to GO's improvement of the

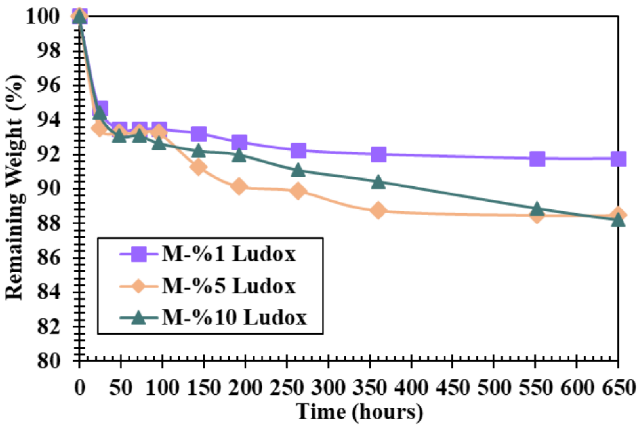

Fig. 13 Hydrolytic stability of Ludox-additive membranes for 650 h at 80°C

SPEEK/PVA membrane in terms of thermal stability [80]. Murmu et al. reported that with the addition of TiO_2, hydrogen bonding between TiO_2 and water molecules occurred and the water uptake capacity increased. They determined the proton conductivity of the SPEEK/PVA/TiO_2 membrane at 110°C as 0.1372 S/cm and attributed the developed proton conductivity to strong hydrogen bonds [79]. The 0.65 S/cm proton conductivity of the M-10% Ludox membrane reported by our study group in this study can compete with the membranes reported in the existing literature and is a proton exchange membrane with high potential.

Hydrolytic Stability

Membranes are of critical importance for the fuel cell, and the failure of a single membrane in a stacked cell directly affects the entire system. For this reason, the lifetime of the fuel cell is linked to the lifetime of the membranes. Membranes are in constant contact with water because they remain moist in order to have high proton conductivity, and water is produced on the cathode side. For these reasons, their water resistance is a measure of the membrane's shelf life. In order to determine the stability of the synthesized membranes in water, hydrolytic stability experiments were carried out at 80°C, which is the operating temperature of PEMFC. The weight losses of the membranes over time as a result of the 650-hour experiments are given in Fig. 13.

It was observed that Ludox-additive membranes retained approximately 88% of their weight after 650 h. It was observed that the membrane with the highest hydrolytic stability belonged to the membrane with 1% Ludox additive by weight, and the hydrolytic stability decreased slightly with increasing Ludox amounts. The main reason why membranes have such high hydrolytic stability is thermal crosslinking. The decreasing void volume and tightening of bonds with thermal crosslinking allow limited water to enter the membrane structure, which creates a hydrolytically stable structure. As can be seen from the water uptake capacities, the amount of water entering the void volume of the membranes increases with the increasing amount of Ludox. This is due to SiO_2's high hydrophilicity [81]. As the density of Ludox, which contains colloidal silica particles, increases in the membrane, it gives the membrane a hydrophilic feature and allows more water passage. The hydroxyl groups in PVA, which have poor stability in water, and the sulfonic acid groups in SPEEK, reduce the hydrolytic stability of the membrane [40]. Parnian et al. reported that SPEEK retained 77% of its weight in a hydrolytic stability experiment conducted with pristine SPEEK at 60°C for 120 h [82]. In a study conducted with TEOS-additive SPEEK-PVA, pristine SPEEK retained 80% of its mass after 120 h, while PVA could only preserve 50% [60]. . In their hydrolytic stability tests with partially fluorinated SPA membranes synthesized by Ying et al., they reported that the membranes with the best hydrolytic stability at 80°C completely dissolved in water in a little more than 24 h [83]. In the hydrolytic stability tests conducted by Akbarian-Feizi et al. with Nafion-117 at 80°C, they stated that the membrane began to shrink after 100 h. The time when Ludox-doped membranes started to shrink was after 350 h [84]. In another study, in the hydrolytic stability experiment performed with Nafion-117, they stated that Nafion-117 lost 1.5% of its weight after 2 h. In the synthesized Ludox-additive membranes, this weight loss occurred within 24 h [85]. The results showed that the hydrolytic stability of Ludox-added membranes was quite high compared to the literature.

Table 1 Oxidative stability of synthesized membranes

	Remaining Weight (%)		
	1 h	3 h	24 h
M-%1 Ludox	92.4	92.4	91.1
M-%5 Ludox	94.5	92.6	91.6
M-%10 Ludox	92.3	89.9	88.8
Nafion-117	99.1	98.4	95.3

Oxidative Stability

Another parameter that determines the membranes' shelf life and fuel cell performance is their oxidative stability. The oxidative stability of membranes provides information about the stability of the membrane structure against possible hydroxyl radicals that may occur in the fuel cell. These hydroxy radicals can attack the membrane matrix and cause the membrane to become dysfunctional. The oxidative stability of the membranes was determined from the weights lost against time at 80°C in the prepared Fenton solution, and the results obtained are given in Table 1.

The weight losses of Ludox-added membranes in Fenton solution vary between approximately 90% and 92.6% after 3 h. At the end of 24 h, weight losses in all membranes remained limited, ranging from 91.6 to 88%. In the oxidative stability tests conducted by Raja et al. at 80°C and using 2 ppm ferrous salt, they reported that pure SPEEK could retain 78.34% of its weight after 24 h [86]. In another study where PVA polymer was used as the main matrix, PVA/KN-B coded membrane lost approximately 20% of its weight after 24 h in 30% H_2O_2 without Fe sources, while PVA/KN-B/DA coded membrane lost approximately 10% [87]. In a study where 3% H_2O_2 and 4 ppm Fe^{+2} by weight were used, pristine SPEEK was completely dissolved in Fenton solution after 24 h, pure PVA after 6 h and SPEEK-PVA after 8 h at 68°C [60]. Despite the high temperature and Fe^{+3} concentration, the synthesized membranes exhibited very high oxidative stability. One of the main reasons for this is thermal crosslinking as well as hydrolytic stability. Free radicals in the environment react with OH^- groups in the PVA chain and free sulfonic acid groups in SPEEK, as a result, the oxidative stability of the membrane decreases [60, 86]. The thermal crosslinking reaction takes place between the hydroxyl groups of PVA and the sulfonic acid groups of SPEEK [40]. As a result of thermal crosslinking, the possibility of free radicals reacting with the membrane decreased as the hydroxyl and sulfonic acid groups in the membrane structure decreased. This increased the oxidative resistance of thermally cross-linked membranes. Another reason is the Ludox density in the structure. While the highest oxidative resistance is obtained with the membrane containing 5% Ludox by mass, the oxidative stability of the membrane containing 10% Ludox decreases slightly. Many studies are show that oxidative resistance increases up to a certain SiO_2-based additive ratio [88]. A higher resistance against hydroxy radicals occurred due to the interaction of SiO_2-SO_3H (sulfonic) groups and Ludox's increase in cross-linking density in the thermal cross-linking reaction. However, after the 5% Ludox additive rate, it is thought that agglomeration occurs, especially as can be seen from mechanical strength tests, and this makes the membrane more vulnerable than others. On the other hand, oxidative stability experiments were carried out with the commercial Nafion-117 membrane, and it was determined that it retained 95.3% of its weight after 24 h. It was observed that although Nafion-117 had better oxidative stability compared to the synthesized membranes, there was no significant difference.

Conclusion

Herein, studies on PEM fuel cells were carried out with SPEEK-PVA blend membranes with Ludox additives in different mass ratios (1%, 5%, and 10%) prepared by the solution casting method. The synthesized membranes were characterized by FTIR, water uptake capacity, swelling property, size change, mechanical strength, ion exchange capacity, AC impedance analysis, hydrolytic resistance, and oxidative stability.

It was determined from FTIR analysis that the Ludox contribution was successfully incorporated into the membrane matrix by the increase in peak intensities in parallel with increasing Ludox amounts. As the amount of Ludox added to the membrane increased from 1 to 10%, there was a 16% enhancement in water uptake capacity. The main reason for this is due to the hydrophilic SiO_2 groups found in the Ludox structure.

With the increasing amount of Ludox, the ion exchange capacity and proton conductivity of the blend membranes increased. The highest ion exchange capacity (1.71 meq/g) and proton conductivity (0.65 S/cm) were obtained for the membrane with a 10% Ludox additive by weight. It was determined that the reason for this increase was due to the strong interaction of SiO_2 and SO_3H groups.

In terms of oxidative resistance and mechanical strength, it was determined that the properties of the membrane deteriorated at rates higher than 5% Ludox additive by weight. While 38.86 MPa tensile stress and 16.2% elongation at break were obtained for the 5% added blend membrane, these values decreased by approximately 21% and 40%, respectively, for the 10% added blend membrane. In addition, the oxidative resistance of the membranes in Fenton solution retained 91.6% of the mass of the membrane with 5% Ludox additive at the end of 24 h, while this value decreased to 88.8% for the membrane containing 10% additive. It was concluded that agglomeration starts to form at the Ludox content of the membrane higher than 5% which causes the decrease in stability in the Fenton solution. All membranes had very high hydrolytic stability and managed to retain approximately 88% of their mass after 650 h at 80°C. The results indicate that the addition of Ludox improves the properties of the membranes, and Ludox-containing structure is considered as a promising matrix composition for PEMFC.

Acknowledgements This Study supported by Gazi University Scientific Research Fund. (FGA-2022-7454).

Author Contributions In this study, all authors were equally and fully involved in every stage of the research process, including conceptualization, methodology, investigation, writing both original draft preparation and review & editing, visualization, and supervision.

Funding Open access funding provided by the Scientific and Technological Research Council of Türkiye (TÜBİTAK).

Data Availability No datasets were generated or analysed during the current study.

Declarations

Competing Interests The authors declare no competing interests.

References

1. Haldar D, Purkait MK (2021) A review on the environment-friendly emerging techniques for pretreatment of lignocellulosic biomass: mechanistic insight and advancements. Chemosphere 264:128523. https://doi.org/10.1016/j.chemosphere.2020.128523
2. Yörük Ö, Zıraman DU, Uysal BZ (2021) Absorption of Sulfur Dioxide by Iron (II) Hydroxide Solution in a multiplate bubble column under magnetic field. Chem Eng Technol 44:1336–1342. https://doi.org/10.1002/ceat.202000123
3. Koçyiğit Çapoğlu İ, Uysal D, Doğan ÖM (2023) Mass transfer studies for CO2 absorption into carbitol acetate as an effective physical absorbent using a laboratory-scale packed column. Heat Mass Transf 1–13. https://doi.org/10.1007/s00231-023-03427-y
4. Öztan H, Çapoğlu İK, Uysal D, Doğan ÖM (2023) A parametric study to optimize the temperature of hazelnut and walnut shell gasification for hydrogen and methane production. Bioresource Technol Rep 23:101581. https://doi.org/10.1016/j.biteb.2023.101581
5. Li Z, Khajepour A, Song J (2019) A comprehensive review of the key technologies for pure electric vehicles. Energy 182:824–839. https://doi.org/10.1016/j.energy.2019.06.077
6. Sazali N, Wan Salleh WN, Jamaludin AS, Mhd Razali MN (2020) New perspectives on fuel cell technology: a brief review. Membranes 10:99. https://doi.org/10.3390/membranes10050099
7. Inal OB, Deniz C (2020) Assessment of fuel cell types for ships: based on multi-criteria decision analysis. J Clean Prod 265:121734. https://doi.org/10.1016/j.jclepro.2020.121734
8. Moorthy S, Sivasubramanian G, Kannaiyan D, Deivanayagam P (2023) Neoteric advancements in polybenzimidazole based Polymer electrolytes for high-temperature proton exchange membrane fuel cells-A versatile review. Int J Hydrog Energy. https://doi.org/10.1016/j.ijhydene.2023.04.005
9. Wang Y, Seo B, Wang B, Zamel N, Jiao K, Adroher XC (2020) Fundamentals, materials, and machine learning of polymer electrolyte membrane fuel cell technology. Energy 1:100014. https://doi.org/10.1016/j.egyai.2020.100014
10. Du L, Prabhakaran V, Xie X, Park S, Wang Y, Shao Y (2021) Low-PGM and PGM-free catalysts for proton exchange membrane fuel cells: stability challenges and material solutions. Adv Mater 33:1908232. https://doi.org/10.1002/adma.201908232
11. Okonkwo PC, Belgacem IB, Emori W, Uzoma PC (2021) Nafion degradation mechanisms in proton exchange membrane fuel cell (PEMFC) system: a review. Int J Hydrog Energy 46:27956–27973. https://doi.org/10.1016/j.ijhydene.2021.06.032
12. Yan X, Xu Z, Yuan S, Han A, Shen Y, Cheng X, Liang Y, Shen S, Zhang J (2022) Structural and transport properties of ultra-thin perfluorosulfonic acid ionomer film in proton exchange membrane fuel cell catalyst layer: a review. J Power Sources 536:231523. https://doi.org/10.1016/j.jpowsour.2022.231523
13. Jamil A, Rafiq S, Iqbal T, Khan HAA, Khan HM, Azeem B, Mustafa M, Hanbazazah AS (2022) Current status and future perspectives of proton exchange membranes for hydrogen fuel cells. Chemosphere 303:135204. https://doi.org/10.1016/j.chemosphere.2022.135204
14. Wu G, Yang Y, Lei Y, Fu D, Li Y, Zhan Y, Zhen J, Teng M (2020) Hydrophilic nano-SiO 2/PVA-based coating with durable antifogging properties. J Coat Technol Res 17:1145–1155. https://doi.org/10.1007/s11998-020-00338-z
15. Wong CY, Wong WY, Loh KS, Daud WRW, Lim KL, Khalid M, Walvekar R (2020) Development of poly (vinyl alcohol)-based polymers as proton exchange membranes and challenges in fuel cell application: a review. Polym Rev 60:171–202. https://doi.org/10.1080/15583724.2019.1641514
16. Altaf F, Gill R, Batool R, Drexler M, Alamgir F, Abbas G, Jacob K (2019) Proton conductivity and methanol permeability study of polymer electrolyte membranes with range of functionalized clay content for fuel cell application. Eur Polymer J 110:155–167. https://doi.org/10.1016/j.eurpolymj.2018.11.027
17. Kim AR, Poudel MB, Chu JY, Vinothkannan M, Santhosh Kumar R, Logeshwaran N, Park B-H, Han M-K, Yoo DJ (2023) Advanced performance and ultra-high, long-term durability of acid-base blended membranes over 900 hours containing sulfonated PEEK and quaternized poly(arylene ether sulfone) in H2/O2 fuel cells. Compos Part B: Eng 254:110558. https://doi.org/10.1016/j.compositesb.2023.110558
18. Sayed Daud SNS, Mohd Norddin MNA, Jaafar J, Sudirman R (2020) High degree sulfonated poly (ether ether ketone) blend with polyvinylidene fluoride as a potential proton-conducting membrane fuel cell. High Perform Polym 32:103–115. https://doi.org/10.1177/095400831985
19. Hu H, Ding F, Ding H, Liu J, Xiao M, Meng Y, Sun L (2020) Sulfonated poly (fluorenyl ether ketone)/Sulfonated α-zirconium phosphate nanocomposite membranes for proton exchange membrane fuel cells. Adv Compos Hybrid Mater 3:498–507. https://doi.org/10.1007/s42114-020-00182-0
20. Al-Othman A, Tremblay AY, Pell W, Letaief S, Burchell TJ, Peppley BA, Ternan M (2010) Zirconium phosphate as the proton conducting material in direct hydrocarbon polymer electrolyte membrane fuel cells operating above the boiling point of water. J Power Sources 195:2520–2525. https://doi.org/10.1016/j.jpowsour.2009.11.052
21. Tawalbeh M, Al-Othman A, Ka'ki A, Farooq A, Alkasrawi M (2022) Lignin/zirconium phosphate/ionic liquids-based proton conducting membranes for high-temperature PEM fuel cells applications. Energy 260:125237. https://doi.org/10.1016/j.energy.2022.125237
22. Li X, Ma H, Wang P, Liu Z, Peng J, Hu W, Jiang Z, Liu B (2019) Construction of high-performance, high-temperature proton exchange membranes through incorporating SiO2 nanoparticles into novel cross-linked polybenzimidazole networks. ACS Appl Mater Interfaces 11:30735–30746. https://doi.org/10.1021/acsami.9b06808
23. Kim AR, Gabunada JC, Yoo DJ (2018) Sulfonated fluorinated block copolymer containing naphthalene unit/sulfonated

polyvinylidene-co-hexafluoropropylene/functionalized silicon dioxide ternary composite membrane for low-humidity fuel cell applications. Colloid Polym Sci 296:1891–1903. https://doi.org/10.1007/s00396-018-4403-y
24. Lee S, Seo K, Ghorpade RV, Nam K-H, Han H (2020) High temperature anhydrous proton exchange membranes based on chemically-functionalized titanium/polybenzimidazole composites for fuel cells. Mater Lett 263:127167. https://doi.org/10.1016/j.matlet.2019.127167
25. Lee KH, Chu JY, Kim AR, Kim HG, Yoo DJ (2021) Functionalized TiO2 mediated organic-inorganic composite membranes based on quaternized poly(arylene ether ketone) with enhanced ionic conductivity and alkaline stability for alkaline fuel cells. J Membr Sci 634:119435. https://doi.org/10.1016/j.memsci.2021.119435
26. Guoa H, Zhangb J, Liua J, Fana S (2023) Facile synthesis of a mixed matrix membrane based on PTA@ MOF-199 nanoparticles with proton conductivity. Digest J Nanomaterials Biostructures 18. https://doi.org/10.15251/DJNB.2023.182.727
27. Khan MI, Shanableh A, Shahida S, Lashari MH, Manzoor S, Fernandez J (2022) SPEEK and SPPO blended membranes for proton exchange membrane fuel cells. Membranes 12:263. https://doi.org/10.3390/membranes12030263
28. Sun C, Negro E, Vezzù K, Pagot G, Cavinato G, Nale A, Bang YH, Di Noto V (2019) Hybrid inorganic-organic proton-conducting membranes based on SPEEK doped with WO3 nanoparticles for application in vanadium redox flow batteries. Electrochim Acta 309:311–325. https://doi.org/10.1016/j.electacta.2019.03.056
29. Hu H, Ding F, Ding H, Liu J, Xiao M, Meng Y, Sun LJ (2020) Sulfonated poly (fluorenyl ether ketone)/Sulfonated α-zirconium phosphate nanocomposite membranes for proton exchange membrane fuel cells. Adv Compos Hybrid Mater 3:498–507. https://doi.org/10.1007/s42114-020-00182-0
30. Seo K, Nam K-H, Han H (2020) Proton transport in aluminum-substituted mesoporous silica channel-embedded high-temperature anhydrous proton-exchange membrane fuel cells. Sci Rep 10:10352. https://doi.org/10.1038/s41598-020-66935-5
31. Wang J, Qu T, Ni J, Cheng F, Hu F, Ou Y, Gong C, Wen S, Chen X, Liu H (2023) Composite Proton exchange membranes based on inorganic proton conductor boron phosphate functionalized multi-walled carbon nanotubes and chitosan. Surf Interfaces 36:102557. https://doi.org/10.1016/j.surfin.2022.102557
32. Ranganathan H, Vinothkannan M, Kim AR, Subramanian V, Oh M-S, Yoo DJ (2022) Simultaneous improvement of power density and durability of sulfonated poly(ether ether ketone) membrane by embedding CeO2-ATiO2: a comprehensive study in low humidity proton exchange membrane fuel cells. Int J Energy Res 46:9041–9057. https://doi.org/10.1002/er.7781
33. Liu L, Pu Y, Lu Y, Li N, Hu Z, Chen S (2021) Superacid sulfated SnO2 doped with CeO2: a novel inorganic filler to simultaneously enhance conductivity and stabilities of proton exchange membrane. J Membr Sci 621:118972. https://doi.org/10.1016/j.memsci.2020.118972
34. Shaari N, Kamarudin SK (2019) Recent advances in additive-enhanced polymer electrolyte membrane properties in fuel cell applications: an overview. Int J Energy Res 43:2756–2794. https://doi.org/10.1002/er.4348
35. Rosli NAH, Loh KS, Wong WY, Lee TK, Ahmad A (2021) Hybrid composite membrane of phosphorylated chitosan/poly (vinyl alcohol)/silica as a proton exchange membrane. Membranes 11:675. https://doi.org/10.3390/membranes11090675
36. Ying YP, Kamarudin SK, Masdar MS (2018) Silica-related membranes in fuel cell applications: an overview. Int J Hydrog Energy 43:16068–16084. https://doi.org/10.1016/j.ijhydene.2018.06.171
37. Guo Z, Chen J, Byun JJ, Cai R, Perez-Page M, Sahoo M, Ji Z, Haigh SJ, Holmes S, M J J o E C (2022) High-performance polymer electrolyte membranes incorporated with 2D silica nanosheets in high-temperature proton exchange membrane fuel cells. 64:323–334. https://doi.org/10.1016/j.jechem.2021.04.061
38. Yagizatli Y, Ulas B, Sahin A, Ar I (2022) Investigation of sulfonation reaction kinetics and effect of sulfonation degree on membrane characteristics for PEMFC performance. Ionics 28:2323–2336. https://doi.org/10.1007/s11581-022-04494-7
39. Mansur HS, Sadahira CM, Souza AN, Mansur AAP (2008) FTIR spectroscopy characterization of poly (vinyl alcohol) hydrogel with different hydrolysis degree and chemically crosslinked with glutaraldehyde. Mater Sci Engineering: C 28:539–548. https://doi.org/10.1016/j.msec.2007.10.088
40. Yagizatli Y, Sahin A, Ar I (2022) Effect of thermal crosslinking process on membrane structure and PEM fuel cell applications performed with SPEEK-PVA blend membranes. Int J Hydrog Energy 47:40445–40461. https://doi.org/10.1016/j.ijhydene.2022.04.183
41. Selvakumar K, Rajendran S, Ramesh Prabhu M (2019) Influence of barium zirconate on SPEEK-based polymer electrolytes for PEM fuel cell applications. Ionics 25:2243–2253. https://doi.org/10.1007/s11581-018-2613-4
42. Candan Karaeyvaz M, Balci S (2021) One pot synthesis of aluminum pillared intercalated layered clay supported silicotungstic acid (STA/Al-PILC) catalysts. Microporous Mesoporous Mater 323:111193. https://doi.org/10.1016/j.micromeso.2021.111193
43. Akti F, Balci S, Dogu T (2019) Effect of synthesis media pH and gel separation technique on properties of copper incorporated SBA-15 catalyst. Mater Chem Phys 236:121776. https://doi.org/10.1016/j.matchemphys.2019.121776
44. Song J, Liao Z, Shi H, Xiang D, Liu Y, Liu W, Peng Z (2017) Fretting wear study of PEEK-Based composites for bio-implant application. Tribol Lett 65:150. https://doi.org/10.1007/s11249-017-0931-8
45. Parnian MJ, Rowshanzamir S, Prasad AK, Advani SG (2018) High durability sulfonated poly (ether ether ketone)-ceria nanocomposite membranes for proton exchange membrane fuel cell applications. J Membr Sci 556:12–22. https://doi.org/10.1016/j.memsci.2018.03.083
46. Tang C-M, Tian Y-H, Hsu S-H (2015) Poly(vinyl alcohol) nanocomposites Reinforced with Bamboo Charcoal Nanoparticles. Mineralization Behavior and Characterization, Materials, pp 4895–4911
47. Liu P, Chen W, Liu C, Tian M, Liu P (2019) A novel poly (vinyl alcohol)/poly (ethylene glycol) scaffold for tissue engineering with a unique bimodal open-celled structure fabricated using supercritical fluid foaming. Sci Rep 9:9534. https://doi.org/10.1038/s41598-019-46061-7
48. Chandraboss V, Kamalakkannan J, Senthilvelan S (2015) Synthesis of AC-Bi@ SiO2 nanocomposite sphere for superior photocatalytic activity towards the photodegradation of malachite green. Can Chem Trans 3:410–429. https://doi.org/10.13179/canchemtrans.2015.03.04.0235
49. Jun M-S, Choi Y-W, Kim J-D (2012) Solvent casting effects of sulfonated poly(ether ether ketone) for polymer electrolyte membrane fuel cell. J Membr Sci 396:32–37. https://doi.org/10.1016/j.memsci.2011.12.008
50. Yang T (2008) Preliminary study of SPEEK/PVA blend membranes for DMFC applications. Int J Hydrog Energy 33:6772–6779. https://doi.org/10.1016/j.ijhydene.2008.08.022
51. Moustafa A, Abd El-Aziz M, Emira H, Rabie A, Essawy H (2014) Pickering emulsion polymerization of styrene using ludox HS-30 as solid particles stabilizer. The dependence on the pH
52. Ganai AK, Bhardwaj R, Hotha S, Gupta SS, Prasad B (2010) Clicking'molecular hooks on silica nanoparticles to immobilize catalytically important metal complexes: the case of gold catalyst immobilization. New J Chem 34:2662–2670. https://doi.org/10.1039/C0NJ00292E

53. Iravani N, Keshavarz M, Taib LA (2023) Acidic ionic liquids immobilized on nano silica sulfuric acid for highly effective catalytic synthesis of 4H-pyrano[2,3-c]pyrazole and dihydropyrano[c] chromene derivatives. Res Chem Intermed 49:4405–4422. https://doi.org/10.1007/s11164-023-05105-4
54. Knauth P, Hou H, Bloch E, Sgreccia E, Di Vona ML (2011) Thermogravimetric analysis of SPEEK membranes: thermal stability, degree of sulfonation and cross-linking reaction. J Anal Appl Pyrol 92:361–365. https://doi.org/10.1016/j.jaap.2011.07.012
55. Hou H, Polini R, Di Vona ML, Liu X, Sgreccia E, Chailan J-F, Knauth P (2013) Thermal crosslinked and nanodiamond reinforced SPEEK composite membrane for PEMFC. Int J Hydrog Energy 38:3346–3351. https://doi.org/10.1016/j.ijhydene.2012.12.019
56. Yang C-C, Chien W-C, Li YJ (2010) Direct methanol fuel cell based on poly(vinyl alcohol)/titanium oxide nanotubes/poly(styrene sulfonic acid) (PVA/nt-TiO2/PSSA) composite polymer membrane. J Power Sources 195:3407–3415. https://doi.org/10.1016/j.jpowsour.2009.12.024
57. Avramov I, Vassilev T, Penkov I (2005) The glass transition temperature of silicate and borate glasses. J Non-cryst Solids 351:472–476. https://doi.org/10.1016/j.jnoncrysol.2005.01.044
58. Lu S-R, Wei C, Yu J-H, Yang X-W, Jiang Y-M (2007) Preparation and characterization of epoxy nanocomposites by using PEO-grafted silica particles as modifier. J Mater Sci 42:6708–6715. https://doi.org/10.1007/s10853-006-1492-7
59. Yagizatli Y, Ar I (2024) Novel Fluoroboric Acid Additive for Blend membrane to be used in PEM fuel cell, characterization studies, and performance test. J Polym Environ. https://doi.org/10.1007/s10924-023-03180-7
60. Sahin A (2018) The development of Speek/Pva/Teos blend membrane for proton exchange membrane fuel cells. Electrochim Acta 271:127–136. https://doi.org/10.1016/j.electacta.2018.03.145
61. Mu'min MS, Komma M, Abbas D, Wagner M, Krieger A, Thiele S, Böhm T, Kerres J (2023) Electrospun phosphonated poly(pentafluorostyrene) nanofibers as a reinforcement of Nafion membranes for fuel cell application. J Membr Sci 685:121915. https://doi.org/10.1016/j.memsci.2023.121915
62. Hooshyari K, Heydari S, Beydaghi H, Rajabi HR (2022) New Nanocomposite membranes based on sulfonated poly (phthalazinone ether ketone) and Fe3O4@ SiO2@ resorcinol–aldehyde–SO3H for PEMFCs. Renewable Energy 186:115–125. https://doi.org/10.1016/j.renene.2021.12.074
63. Wang Z, Zhang J, Lu S, Xiang Y, Shao Z, Jiang SP (2024) Stability and performance of in-situ formed phosphosilicate nanoparticles in phosphoric acid-doped polybenzimidazole composite membrane fuel cells at elevated temperatures. Int J Hydrogen Energy 57:918–928. https://doi.org/10.1016/j.ijhydene.2024.01.095
64. Zheng C, Xie N, Liu X, Wang L, Zhu W, Pei Y, Yue R, Liu H, Yin S, Yao J, Zhang J, Yin Y, Guiver MD (2024) Durability improvement of proton exchange membrane fuel cells by doping silica–ferrocyanide antioxidant. J Membr Sci 690:122195. https://doi.org/10.1016/j.memsci.2023.122195
65. Morales J, Michell RM, Sommer-Márquez A, Rodrigue D (2023) Effect of Biobased SiO2 on the Morphological, Thermal, Mechanical, Rheological, and Permeability properties of PLLA/PEG/SiO2 biocomposites. J Compos Sci
66. Badami AS, Lane O, Lee H-S, Roy A, McGrath JE (2009) Fundamental investigations of the effect of the linkage group on the behavior of hydrophilic–hydrophobic poly (arylene ether sulfone) multiblock copolymers for proton exchange membrane fuel cells. J Membr Sci 333:1–11. https://doi.org/10.1016/j.memsci.2008.12.066
67. Murmu R, Roy D, Patra SC, Sutar H, Senapati P (2022) Preparation and characterization of the SPEEK/PVA/Silica hybrid membrane for direct methanol fuel cell (DMFC). Polym Bull 1–27. https://doi.org/10.1007/s00289-021-03602-3
68. Wu Y, Wu C, Varcoe JR, Poynton SD, Xu T, Fu Y (2010) Novel silica/poly (2, 6-dimethyl-1, 4-phenylene oxide) hybrid anion-exchange membranes for alkaline fuel cells: Effect of silica content and the single cell performance. J Power Sources 195:3069–3076. https://doi.org/10.1016/j.jpowsour.2009.11.118
69. Ying Y, Kamarudin S, Masdar M (2018) Silica-related membranes in fuel cell applications: an overview. Int J Hydrog Energy 43:16068–16084. https://doi.org/10.1016/j.ijhydene.2018.06.171
70. Jesuraj K, Manimuthu RP (2019) Preparation and characterization of hybrid chitosan/PEO–silica membrane doped with phosphotungstic acid for PEM fuel cell application. Polymer-Plastics Technol Mater 58:14–30. https://doi.org/10.1080/03602559.2018.1455862
71. Cortés FB, Chejne F, Carrasco-Marín F, Pérez-Cadenas AF, Moreno-Castilla C (2012) Water sorption on silica-and zeolite-supported hygroscopic salts for cooling system applications. Energy Conv Manag 53:219–223. https://doi.org/10.1016/j.enconman.2011.09.001
72. Safronova EY, Yaroslavtsev AB (2012) Nafion-type membranes doped with silica nanoparticles with modified surface. Solid State Ionics 221:6–10. https://doi.org/10.1016/j.ssi.2012.05.030
73. Horvat CI, Zhu X, Türp D, Vinokur RA, Demco DE, Fechete R, Conradi O, Graichen A, Anokhin D, Ivanov DA, Möller M (2012) Perfluorosulfonic acid ionomer – silica composite membranes prepared using hyperbranched polyethoxysiloxane for polymer electrolyte membrane fuel cells. Int J Hydrog Energy 37:14454–14462. https://doi.org/10.1016/j.ijhydene.2012.07.014
74. Dresch MA, Isidoro RA, Linardi M, Rey JF, Q, Fonseca FC, Santiago EI (2013) Influence of sol–gel media on the properties of Nafion–SiO2 hybrid electrolytes for high performance proton exchange membrane fuel cells operating at high temperature and low humidity. Electrochim Acta 94:353–359. https://doi.org/10.1016/j.electacta.2012.09.036
75. Xie L, Cho E-B, Kim D (2011) Sulfonated PEEK/cubic (Im3m) mesoporous benzene–silica composite membranes operable at low humidity. Solid State Ionics 203:1–8. https://doi.org/10.1016/j.ssi.2011.09.007
76. Han SY, Park J, Kim D (2013) Proton-conducting electrolyte membranes based on organosiloxane network/sulfonated poly(ether ether ketone) interpenetrating polymer networks embedding sulfonated mesoporous benzene–silica. J Power Sources 243:850–858. https://doi.org/10.1016/j.jpowsour.2013.06.072
77. Yang C-C, Li YJ, Liou T-H (2011) Preparation of novel poly(vinyl alcohol)/SiO2 nanocomposite membranes by a sol–gel process and their application on alkaline DMFCs. Desalination 276:366–372. https://doi.org/10.1016/j.desal.2011.03.079
78. Murmu R, Roy D, Patra SC, Sutar H, Senapati P (2022) Preparation and characterization of the SPEEK/PVA/Silica hybrid membrane for direct methanol fuel cell (DMFC). Polym Bull 79:2061–2087. https://doi.org/10.1007/s00289-021-03602-3
79. Murmu R, Sutar H (2018) A Novel SPEEK-PVA-TiO 2 Proton conducting Composite membrane for PEMFC operations at elevated temperature. J Polym Mater 35. https://doi.org/10.32381/JPM.2018.35.04.2
80. Reyes-Rodriguez JL, Escorihuela J, García-Bernabé A, Giménez E, Solorza-Feria O, Compañ V (2017) Proton conducting electrospun sulfonated polyether ether ketone graphene oxide composite membranes. RSC Adv 7:53481–53491. https://doi.org/10.1039/C7RA10484G
81. Xu B, Zhang Q (2021) Preparation and properties of hydrophobically modified nano-SiO2 with hexadecyltrimethoxysilane. ACS Omega 6:9764–9770. https://doi.org/10.1021/acsomega.1c00381
82. Parnian MJ, Gashoul F, Rowshanzamir S (2017) Studies on the SPEEK membrane with low degree of sulfonation as a stable proton exchange membrane for fuel cell applications. Hydrogen

Fuel Cell Energy Storage 3:221–232. https://doi.org/10.22104/IJHFC.2017.428
83. Chang Y, Lee Y-B, Bae C (2011) Partially fluorinated sulfonated poly (ether amide) fuel cell membranes: influence of chemical structure on membrane properties. Polymers 3:222–235. https://doi.org/10.3390/polym3010222
84. Akbarian-Feizi L, Mehdipour-Ataei S, Yeganeh H (2010) Survey of sulfonated polyimide membrane as a good candidate for nafion substitution in fuel cell. Int J Hydrog Energy 35:9385–9397. https://doi.org/10.1016/j.ijhydene.2010.03.072
85. Liaqat K, Fazil S, Rehman W, Saeed S, Menaa F, Shah SA, Nawaz M, Alharbi WN, Menaa B, Farooq M (2021) Sulfonated polyimide membranes derived from a Novel Sulfonated Diamine. with Pendant Benzenesulfonic Acid for Fuel Cells, Energies
86. Raja K, Raja Pugalenthi M, Ramesh Prabhu M (2020) The effect of incorporation of ferrous titanate nanoparticles in sulfonated poly (ether ether ketone)/poly (amide imide) acid-base polymer for cations exchange membrane fuel cells. J Solid State Electrochem 24:35–44. https://doi.org/10.1007/s10008-019-04453-9
87. Zhou T, Li Y, Wang W, He L, Cai L, Zeng C (2019) Application of a novel PVA-based proton exchange membrane modified by reactive black KN-B for low-temperature fuel cells. Int J Electrochem Sci 14:8514–8531. https://doi.org/10.20964/2019.09.16
88. Modau L, Sigwadi R, Mokrani T, Nemavhola F (2023) Chitosan Membranes for direct methanol fuel cell applications. Membranes 13:838. https://doi.org/10.3390/membranes13100838

Authors and Affiliations

Yavuz Yagizatli[1] · Berdan Ulas[2] · Alpay Sahin[1] · Irfan Ar[1]

✉ Yavuz Yagizatli
yavuzyagizatli@gazi.edu.tr

[1] Graduate School of Natural and Applied Sciences, Faculty of Engineering, Department of Chemical Engineering, Gazi University, Eti Mahallesi, Yükseliş Sokak, No:5, Room,544 Maltepe, Ankara 06570, Turkey

[2] Faculty of Engineering, Department of Mining Engineering, Van Yüzüncü Yıl University, Bardakçı Mahallesi, Yüzüncü Yıl Üniversitesi Kampüsü, Tuşba, Van 65080, Turkey